JOURNAL OF SPACECRAFT AND ROCKETS
Vol. 45, No. 5, September–October 2008

Dynamic Impact Tolerance of Space Shuttle Orbiter Wing Leading-Edge Panels

Edwin L. Fasanella,* Karen E. Jackson,* Karen H. Lyle,† Lisa E. Jones,† Robin C. Hardy,‡ and Sotiris Kellas†
NASA Langley Research Center, Hampton, Virginia 23681
and
Kelly S. Carney§ and Matthew E. Melis§
NASA John H. Glenn Research Center at Lewis Field, Cleveland, Ohio 44135

DOI: 10.2514/1.31373

This paper describes a research program conducted to enable accurate prediction of the impact tolerance of the shuttle Orbiter leading-edge wing panels using physics-based codes such as LS-DYNA, a nonlinear explicit transient dynamic finite element code. The shuttle leading-edge panels are constructed of reinforced carbon–carbon composite material, which is used because of its thermal properties to protect the shuttle during reentry into the Earth's atmosphere. Accurate predictions of impact damage from insulating foam and other debris strikes that occur during launch require materials characterization of expected debris, including strain-rate effects. First, analytical models of individual foam and reinforced carbon–carbon materials were validated. Next, analytical models of foam cylinders impacting 6 × 6 in. reinforced carbon–carbon flat plates were developed and validated. LS-DYNA pretest models of the reinforced carbon–carbon flat-plate specimens established the impact velocity of the test for three damage levels: no detectable damage, nondestructive-evaluation-detectable damage, or visible damage such as a through-the-thickness crack or hole. Finally, the threshold of impact damage for reinforced carbon–carbon on representative Orbiter wing panels was predicted for both a small through-the-thickness crack and for nondestructive-evaluation-detectable damage.

I. Introduction

DURING the investigation by the Columbia Accident Investigation Board (CAIB), the NASA Johnson Space Center's Orbiter Project Office requested various teams from industry, academia, national laboratories, and NASA to apply physics-based analyses to characterize the expected damage to the shuttle thermal protection system tiles and reinforced-carbon–carbon (RCC) material for high-speed foam impacts. The forensic evidence from the Columbia debris assessment study eventually led investigators to conclude that the breach to the shuttle Orbiter thermal protection system was caused by a block of BX-250 external tank insulating foam that was released from the bipod ramp area and that impacted and penetrated the lower portion of a left-wing leading-edge RCC panel (see Fig. 1). The location of the impact was determined to be the left-wing RCC panel 8. Consequently, the CAIB sanctioned a foam-impact test onto an RCC panel 8 in July 2003 at the Southwest Research Institute (SwRI). In the test, a 1.67-lb block of foam was shot from a large compressed-air gun and impacted panel 8 at a velocity of 777 ft/s at an angle of incidence of 25.1 deg in an attempt to simulate the scenario observed approximately 82 s into Columbia's flight. The impact resulted in a large 16 × 16 in. hole in panel 8. Figure 1b shows the relative locations of the RCC panels of interest on the left wing, including panels 6, 8, and 9.

A. Accident Investigation and Return-to-Flight Activities

Chapter 11 recommendation 3.3-2 of the CAIB report [1] requested that NASA initiate a program to improve the impact resistance of the wing leading edge. The second part of the recommendation was for NASA to determine the actual impact resistance of current materials and the effect of likely debris strikes. In addition, recommendation 3.8.2 states,

> Develop, validate, and maintain physics-based computer models to evaluate thermal protection system damage from debris impacts. These tools should provide realistic and timely estimates of any impact damage from possible debris from any source that may ultimately impact the Orbiter. Establish impact damage thresholds that trigger responsive correction action, such as on-orbit inspection and repair, when indicated.

During the shuttle Return-to-Flight (RTF) program, a team from NASA John H. Glenn Research Center at Lewis Field (GRC), NASA Langley Research Center (LaRC), and Boeing Philadelphia was given the following task: Develop a validated finite element model of the Orbiter wing leading edge that is capable of accurately predicting the threshold of critical damage (the shuttle could not safely return) from debris (including foam, ice, and ablators) for a variety of impact conditions. The nonlinear dynamic finite element code LS-DYNA [2] was chosen as the tool to build these models. The definition of the threshold of damage has evolved as knowledge of impact damage has progressed. Initially, all LS-DYNA models for both foam- and ice-debris impacts used a threshold of damage defined to be a small through-the-thickness crack, which was defined as from one to five RCC shell elements deleted using a progressive failure criteria based on strain. However, the current definition of the RCC threshold of damage is "any damage detectable by nondestructive-evaluation (NDE) testing." This definition is not as easy to correlate with LS-DYNA predictions as the through-crack. Critical RCC damage is currently defined as sufficient front-side silicon carbide (SiC)

Presented as Paper 3631 at the AIAA Jet Propulsion Conference, Tucson, AZ, 10–13 July 2007; received 2 April 2007; revision received 21 November 2007; accepted for publication 3 December 2007. This material is declared a work of the U.S. Government and is not subject to copyright protection in the United States. Copies of this paper may be made for personal or internal use, on condition that the copier pay the $10.00 per-copy fee to the Copyright Clearance Center, Inc., 222 Rosewood Drive, Danvers, MA 01923; include the code 0022-4650/08 $10.00 in correspondence with the CCC.

*Senior Aerospace Engineer, Structural Dynamics Branch. Associate Fellow AIAA.
†Senior Aerospace Engineer, Structural Dynamics Branch.
‡Senior Aerospace Engineer, Structural Dynamics Branch. Senior Member AIAA.
§Senior Aerospace Engineer, Structural Mechanics and Dynamics Branch. Member AIAA.

coating loss plus internal RCC delamination that is likely to produce burn-through of the leading edge, resulting in an unsafe reentry. The critical outer surface of the RCC was treated to produce SiC to protect the carbon from oxidation at the high reentry temperatures [3]. Since the CAIB report was released, the team has been developing LS-DYNA models of the RCC leading-edge panels, conducting detailed materials-characterization tests to obtain dynamic material-property data for RCC and debris, and correlating the LS-DYNA models with data obtained from impacts tests for both small-scale flat panels and full-size RCC flight hardware panels [4–9].

Full-scale impact testing of shuttle RCC leading-edge wing panels is quite expensive. Although practice shots were made onto replica fiberglass wing leading-edge panels from the Orbiter Enterprise, only two full-scale tests were performed on RCC wing leading-edge panels during the CAIB investigation. The first RCC test was a foam impact onto leading-edge panel 6 in June 2003, which produced only an edge crack. Then, in July 2003, the foam impact onto panel 8 produced a 16-in.-wide hole.

In September 2003, three tests of increasing severity were performed in which foam projectiles were repeatedly shot onto the same RCC panel 9L in the apex region. From LS-DYNA analyses, the apex region with the highest debris incidence angle (about 45 deg) was predicted to be more vulnerable than the lower surface. The full-scale panels require a long lead time to manufacture, and there are also only a small number of spare panels available. Obviously, there are not enough panels or resources to test all 22 RCC wing panels for a test matrix of different sizes of debris traveling at expected impact velocities and striking each panel at multiple locations. However, a sufficient number of tests are absolutely necessary to characterize the damage threshold for the RCC panels. For RTF, only foam- and ice-debris impacts were analyzed. Some foam debris is expected for the redesigned tank, and ice is the second most likely type of debris.

The foam that brought down Columbia was an abnormally large 1.67-lb wedge of hand-applied foam from the bipod ramp area in which the external tank is attached to the Orbiter (see Fig. 1). The normal foam-debris environment consists of small pieces, each typically only a fraction of a pound. The foam wedge was estimated to impact the left wing of the Orbiter at a velocity of over 700 ft/s. Although the bipod ramp area was redesigned to use heaters, thus eliminating the large piece of hand-applied foam that doomed Columbia, smaller foam debris can still potentially cause serious damage if the impact is at a high velocity at a relatively large incidence angle. According to debris transport analysts, a small piece of foam shed from the external tank stops very quickly in the slipstream, allowing the foam to impact the Orbiter at velocities as high as 2500 ft/s.

B. Dynamic Material Characterization

In addition to experimental tests of debris impacting RCC, which are needed to validate LS-DYNA models, tests are also needed to determine the dynamic material properties of the foam, ice, and ablators. These tests are required to develop the physics-based material models for LS-DYNA that include strain-rate data. Much of the high-speed crush testing of foam, ice, and ablators required to develop these LS-DYNA material models was generated using a high-speed bungee-assisted drop tower at LaRC, shown in Fig. 2.

C. Model Validation

This paper documents the LS-DYNA modeling of foam-debris impacts onto RCC and will present the test-analysis correlations for both subscale and full-scale debris impacts. Validation occurred at three different levels. Level-1 testing was performed to validate the foam and RCC models. Level-1 tests of foam impacts onto a rigid backstop instrumented with a load cell were conducted to validate the foam model. A series of three-point bend tests were performed as part of the level-1 validation of the RCC model. Level-2 validation tests included small foam cylinders that were impacted onto 6×6 in. RCC flat plates. Level-3 tests were full-scale tests and included impact tests of Orbiter wing panels 6, 8, and 9 that were performed at SwRI. Tests of panel 9 for both foam and ice impacts were conducted in late 2004 and early 2005. The validated RCC and foam material models were used to provide the test engineer with the test impact velocity for each desired damage state. Some of the RCC damage states in order of severity included the following: 1) no damage, meaning no-visible surface damage and no NDE-detectable damage; 2) NDE-detectable internal damage to the RCC, and 3) a through-the-thickness crack or a hole. NDE techniques used to evaluate the RCC leading edge after each shuttle flight include eddy-current sensors to detect cracks, thermography to detect internal damage such as delamination, and ultrasonic testing. The test setup, model description, and test-analysis correlation will be presented in the following sections of the paper for each different test configuration and level.

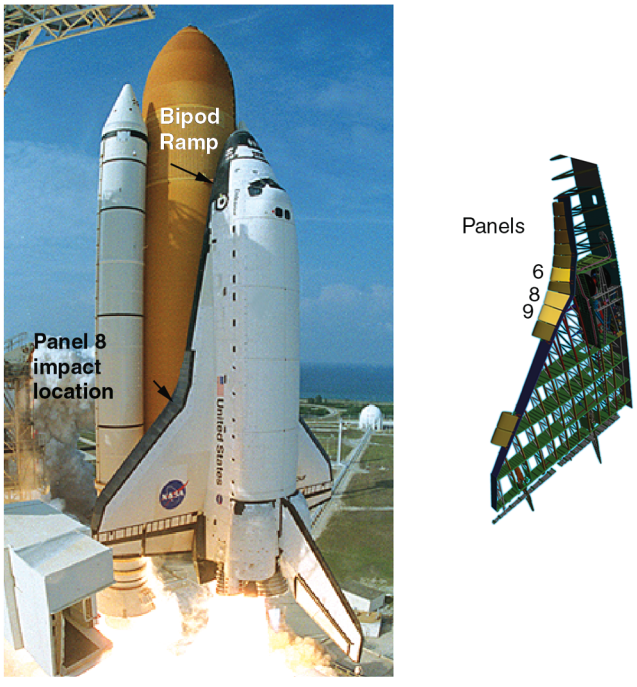

Fig. 1 Picture of Columbia at liftoff and schematic of the left wing showing the wing panels of interest.

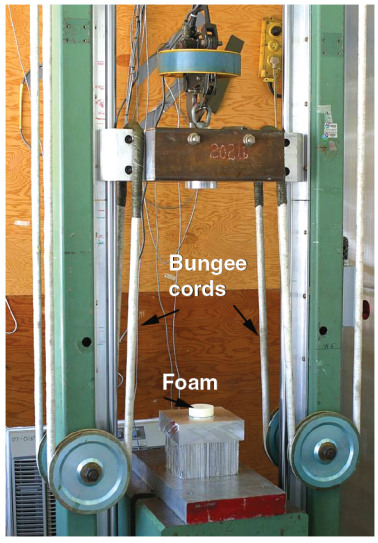

Fig. 2 One configuration of the high-speed bungee-assisted drop tower showing the foam disk before impact.

II. Level-1 Validation Tests

The two level-1 material-model validation tests are described next. First, quasi-static three-point bending tests were conducted on small RCC specimens. The second level-1 tests validated the dynamic foam model and consisted of a ballistic impact of foam onto a rigid backstop.

A. Test Setup: RCC Three-Point Bend

Southern Research Institute (SRI) cut 20 RCC specimens for three-point bend testing plus a compression test coupon, a tension test coupon, and a scrap for testing the coating crush strength from RCC test panel TC3-11. Static (0.1 in./min loading) and low-rate (20 in./min) dynamic three-point bend tests of 19-ply RCC coupons, 1.0 in. wide by 5.8 in. long (5.25-in. gauge length), were conducted with incremental loading and NDE after each load cycle to validate the LS-DYNA RCC threshold of damage predictions [10]. The objectives of the tests were 1) to study the damage initiation and propagation in the RCC samples under quasi-static three-point bend loading, 2) to determine the NDE-detectable damage threshold, 3) to correlate first-detectable NDE damage with LS-DYNA damage parameters, and 4) to determine if internal damage or delamination can be initiated in RCC bend tests, and if so, can that damage be correlated with LS-DYNA damage parameters. A picture of the test setup is shown in Fig. 3a, and a failed specimen is shown in Fig. 3b. The rectangular blocks to the left and right of center on top of the specimen are acoustic sensors.

B. Model Description: Three-Point Bend Test

SRI performed material testing on the tension and compression test coupons that were cut from the same panel as the three-point bend coupons. SRI provided the complete stress–strain curves to failure that were used as input into the LS-DYNA Mat-58 material model [11,12]. For all RCC models, Mat 58 (Mat laminated composite fabric) with failure was used as the material model for the RCC. The RCC material parameters required for input are based on available RCC material data obtained by coupon-testing to failure of laminates of varying thickness in both tension and compression. During testing, it was found that there is a wide variation in the RCC material properties for as-fabricated material. A continuum damage model is used in the Mat-58 formulation to simulate internal damage with increasing load, which weakens the material and produces the nonlinear stress–strain curves for tension and compression. The damage parameter starts out at zero and approaches one at failure. By adjusting the initial moduli, strength, and maximum strain values and post-maximum-strength (strain-softening) parameters SLIMC for compression and SLIMT for tension, the experimental stress–strain curves can be matched to a reasonable degree [4]. Although RCC stress–strain curves have different Young's moduli in tension and compression, the initial modulus in compression was used in the simulations. The RCC was modeled as 19 plies with alternating $\pm$90-deg orientations. The outer layer of SiC that protects the carbon–carbon substrate from oxidation was not specifically modeled. Instead, each individual ply was modeled using the smeared laminate properties. Other important RCC parameters include the strength in tension, compression, and shear and the corresponding strains SLIMC and SLIMT, plus an element erosion parameter or failure strain, ERODS, that must be empirically determined. If ERODS is too small, the material will fail too early. If ERODS is too large, the material will fail too late and will deform too much. From an early study of foam impacting simply supported RCC coupons, an ERODS value of 0.1 gave reasonable results and was used in this model. The ERODS, SLIMC, and SLIMT parameters used in Mat 58 have remained fixed since late 2003. Because the RCC material properties vary considerably, six standardized RCC models were constructed: minimum-, average-, and maximum-strength as-fabricated and minimum-, average-, and maximum-strength flight-degraded. In addition, these six different models had to be constructed for each of the different RCC thicknesses. For 19 plies, 0.233 in. was the nominal RCC thickness.

Other RCC damage modes of concern are front-surface SiC coating loss plus internal RCC delamination. Such damage had been noted to produce complete burn-through of small RCC flat panels that were subjected to arc-jet testing. Also, the smeared laminate LS-DYNA model does not directly predict either coating loss or delamination. It was speculated that if delamination occurred early in the three-point bend test, then the damage parameters that are generated by the Mat-58 RCC material model could be correlated with the onset of RCC delamination. If no delamination occurred, then the Mat-58 damage parameters would be calibrated to first-detectable NDE damage for the three-point bend test, which is a one-dimensional test with simple boundary conditions.

The model discretization (580 shell elements) is shown in Fig. 4. The load was spread over nine nodes at the center and simple-support boundary conditions were applied at the ends at the positions of the two rollers (see Fig. 3a).

C. Test-Analysis Correlation: Three-Point Bend Test

Because Mat 58 is not implemented in the implicit version of LS-DYNA that one would ordinarily use for a static simulation, a dynamic simulation was performed slowly, such that the kinetic energy was negligible when compared with the strain energy in the RCC flex specimen. It was found that a total load of 145 lb applied linearly in time over 0.03 s gave reasonable results. The Mat-58 damage parameter in the X direction (see Fig. 4), which is called history variable 1 in the LS-DYNA output file, is shown in Fig. 5 for each of the 19 layers vs time for shell element 296 located near the center of the specimen. In the stacking sequence, a single integration point was assigned for each of the 19 plies. The damage parameter is largest for the bottom ply labeled J, which is experiencing the maximum tension. The ply next to the bottom layer is labeled A, the center ply is O, and the top ply, which is in maximum compression, is denoted by S. Note that RCC is approximately twice as strong in compression as in tension. Also, the stress–strain curve in tension is highly nonlinear. Thus, the center ply is not the neutral axis. The history variable in the X direction increases dramatically around 0.025 s, which is at a load of about 120 lb. Failure was noted to occur in the tests between 128–130 lb, which was well predicted, as shown in Fig. 6, in which the bottom-layer damage parameter is plotted vs the applied load. The first damage in the form of surface cracks was not detected by eddy current until about 120 lb, which corresponds to a damage parameter greater than 0.9, as shown in Fig. 6. Complete failure of the specimen was predicted for a damage parameter of 1, which corresponds to 129 lb in Fig. 6 . The initial failure for the bend tests was always a tension crack in the lower ply, as depicted in Fig. 3b. Complete failure then rapidly occurred. Internal damage or

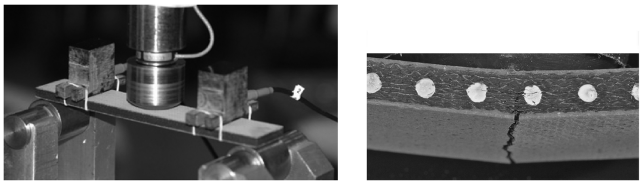

a) Bend test setup

b) RCC bend specimen showing crack initiation

Fig. 3 Level-1 three-point bend test of the RCC coupon (white dots on the right are for photogrammetry).

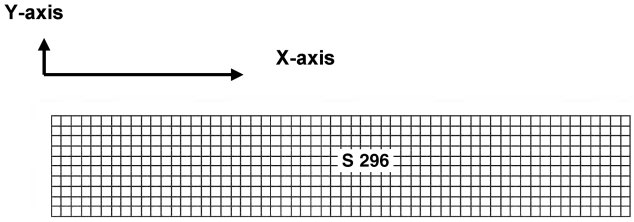

Fig. 4 Simple three-point specimen discretization with shell S 296 near the center.

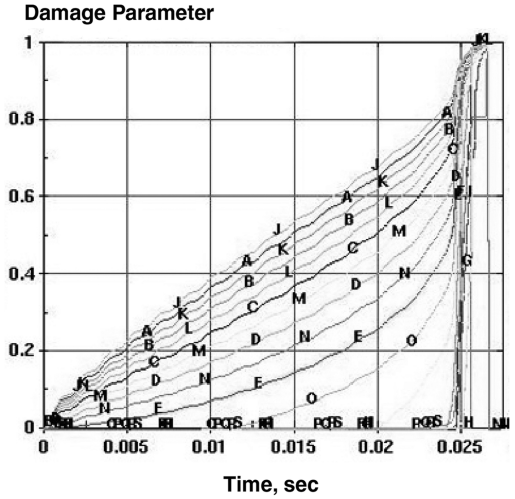

Fig. 5 LS-DYNA damage parameter vs time for each ply of the center shell element 296. The load was applied linearly with time; a time of 0.025 s corresponds to a load of 120 lb.

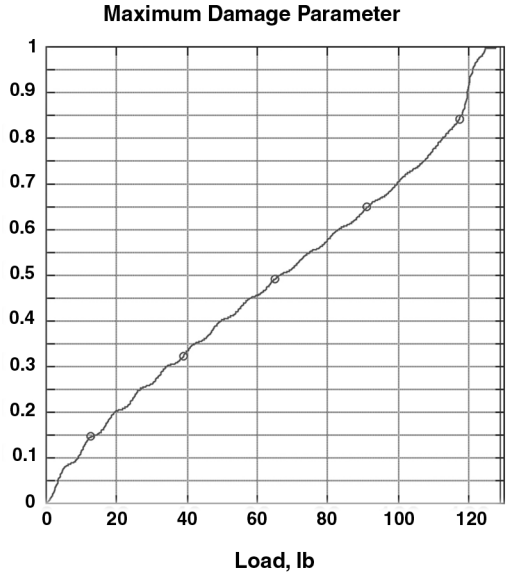

Fig. 6 Maximum damage parameter vs load (bottom ply).

delamination typically did not occur. If delamination did occur, it occurred very late in the loading sequence at the time of failure. No internal damage was detected by any NDE technique before complete failure. NDE techniques vary in their ability to detect internal damage. Typically, ultrasonics proved to be more sensitive than thermography in detecting RCC internal damage.

D. Test Setup: Foam Ballistic Impact

Data from a series of ballistic impact tests of foam that were conducted at GRC, along with high-speed foam-impact data from drop-tower tests performed at LaRC, were used to generate BX-250 and BX-265 foam models. Both foams are polyurethane-based and are used to insulate the cryogenic external tank. The fluorinated hydrocarbon blowing agent originally used for BX-250 was recently changed to a more environmentally friendly gas for BX-265. Although the foams are very similar, their crush behavior differs slightly, with the BX-265 properties being more dependent on temperature. The GRC ballistic test consisted of shooting a 1.25×3.0 in. cylindrical foam projectile onto an aluminum plate instrumented with load cells [4]. The aluminum plate was oriented at angles of 10, 15, 23, and 90 deg. The foam-projectile speeds were approximately 700 and 800 ft/s.

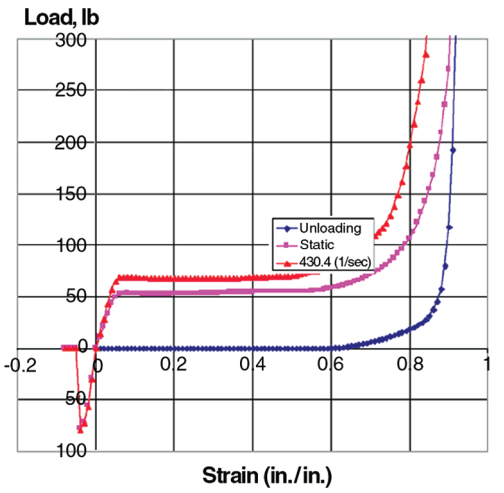

Fig. 7 Foam model for BX-265 in the rise direction at room temperature; tension is negative.

E. Model Description: Foam Ballistic Impact

The external-tank foam material representation for the projectile used the LS-DYNA Mat-83 Fu Chang foam model [8]. Strain-rate effects were found to be important in the foam material at the velocities of interest. The external-tank foam is a closed-cell polyurethane foam that is sprayed onto the tank in layers. The material strength is direction-dependent, with the rise direction having the greatest crush strength. High-strain-rate data for the Fu Chang model were generated in a specially configured and instrumented 14-ft bungee-assisted drop tower at the Impact Dynamics Research Facility at LaRC that can achieve strain rates of over 400/s (see Fig. 2). The test specimens of BX-250 (or BX-265) foam were short cylinders, nominally 2.5 in. in diameter and 1.375 in. tall. A drop in head velocity exceeding 600 in/s was required to produce strain rates over 400/s. The high-strain-rate data were directly input into the Fu Chang model. Different foam models were created for different orientations and for different temperatures. A series of curves input for the BX-265 room-temperature foam model is shown in Fig. 7. The data curves for the various strain rates must be aggressively smoothed and must not overlap. Also, the exponential compaction portion of each curve must be captured to very high stress levels to prevent the solid foam elements from turning inside-out and forming negative volumes. A negative volume error immediately stops LS-DYNA program execution. The unloading curve is input as the unloading for the lowest strain rate (in this case, the static curve).

A typical simulation of a test modeled in LS-DYNA is shown in Fig. 8. Both the projectile and target were modeled using solid elements, and the stiffnesses of the load cells were represented as springs.

F. Test-Analysis Correlation: Foam Ballistic Impact

The qualitative behavior of the foam analytical model, shown in Figs. 8b and 8c, showed excellent agreement with high-speed video of the test. The simulation picked up the maximum compression and also captured the tension failure of the foam in rebound. A comparison of experimental and analytical resultant forces is plotted in Fig. 9. Excellent agreement was obtained.

III. Level-2 Validation Tests

A. Test Setup: Flat Plates

A series of tests were conducted at GRC, starting in June 2004, in which a cylindrical foam projectile impacted 6×6 in. RCC flat panels. The panels had 19 plies with a nominal total thickness of 0.233 in. Foam-impact tests were conducted at a normal (90-deg) incidence angle to the panel and at a 45-deg incidence angle. The foam was shot from an air gun into a vacuum box that contained the framed panel. The panel was restrained around the perimeter by

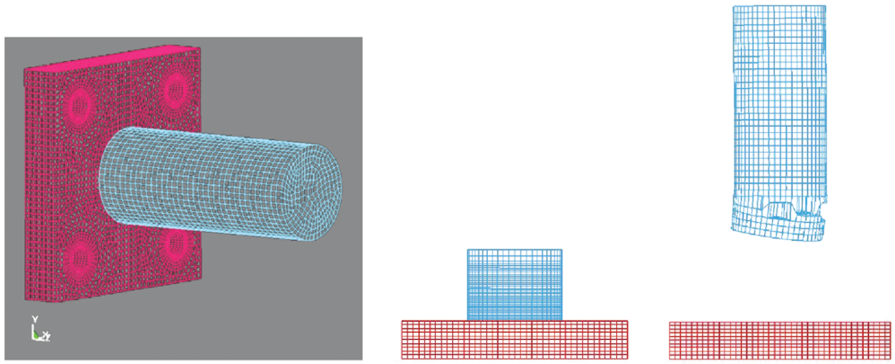

a) Foam at impact onto load cell b) Maximum compression c) Foam rebounding with failures

Fig. 8 Typical LS-DYNA model of foam impacting an instrumented target.

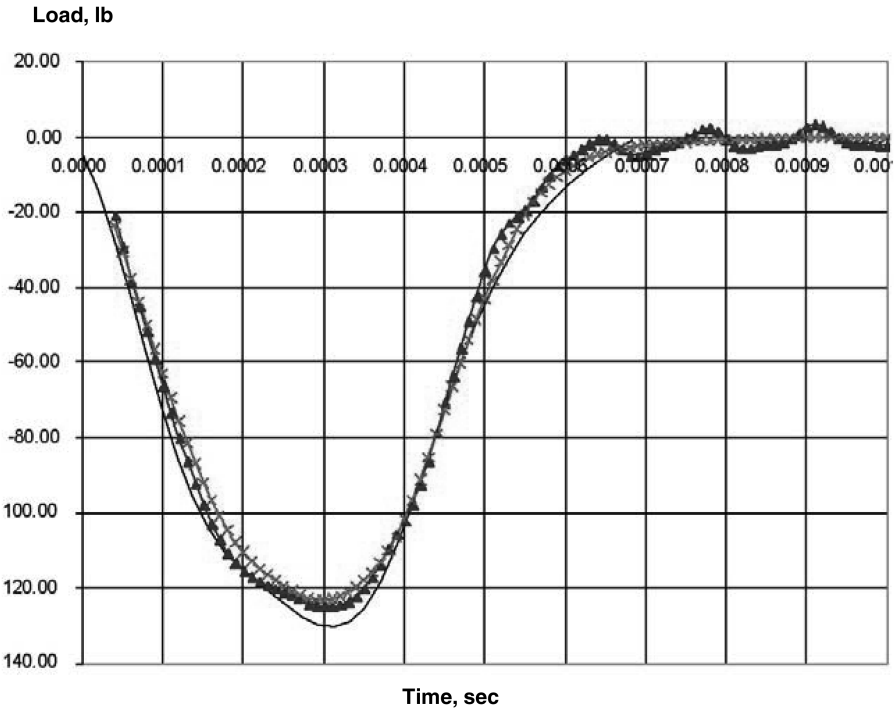

Fig. 9 Comparison of test data (black line) with analysis (triangles and crosses) for a 23-deg impact at 693 ft/s.

0.375-in.-diam half-round aluminum rods that framed the specimen. A posttest photograph of the back side of one of the panels is shown in Fig. 10. Some back-side coating loss is evident. Because the RCC must preserve its SiC coating to survive reentry, any coating loss on the front side of the panel is significant. The speckle finish on the back side of the panel is a sprayed-on pattern that is used by the Aramis photogrammetric measurement tool. High-speed video cameras were used in conjunction with software to determine the displacement of the panel in three dimensions.

The tests were conducted according to procedures developed when the onset of RCC damage was specified as a through-the-thickness crack. For this reason, most of the impacts produced damage that exceeded the updated threshold using the onset of NDE-detectable damage. Only the results for the 45-deg impacts are included in this section, because

1) More impacts at the new threshold defined as the onset of NDE-detectable damage exist for 45-deg impacts.

2) A glancing impact is much more likely than a normal impact, based on debris transport results.

Results for 90-deg impacts can be found in [9].

The 45-deg test configuration including a foam projectile just before impact is shown in Fig. 11. In each test, the RCC panel had dimensions 5.95×5.95 in., with a nominal thickness of 0.233 in. The plate thicknesses were observed to vary from 0.21 to 0.24 in. Experimentally, the panels were constrained on the upper and lower surfaces, with 0.375-in.-diam aluminum half-round rods located 0.16 in. from the four edges. The BX-265 foam projectiles were nominally 1.5 in. in diameter and 3.0 in. long, with a weight of 0.007 lb (3.0-g mass). The following information was acquired for each test: impact velocity, pre- and posttest photographs, pre- and posttest nondestructive evaluations, and dynamic displacements using the Aramis photogrammetry system.

B. Model Description: Flat Plates

A typical model of an LS-DYNA simulation of the impact of a 1.25-in.-diam foam cylinder onto a 6×6 in. flat plate of 19-ply RCC material is shown in Fig. 12. Various boundary conditions were simulated to bound the actual response. The flat plate was restrained at 0.1625 in. from the edges by round aluminum rods in a picture-frame configuration. Thus, the nominal dimensions of the model were 5.675×5.675 in. The units used in the LS-DYNA model for length, mass, and time were inches, $\text{lb} \cdot \text{s}^2/\text{in.}$, and seconds. The RCC plate was 6×6 in., with a shell-element edge length of 0.1 in. Idealized boundary conditions were applied at the locations matching the test. Specifically, the out-of-plane

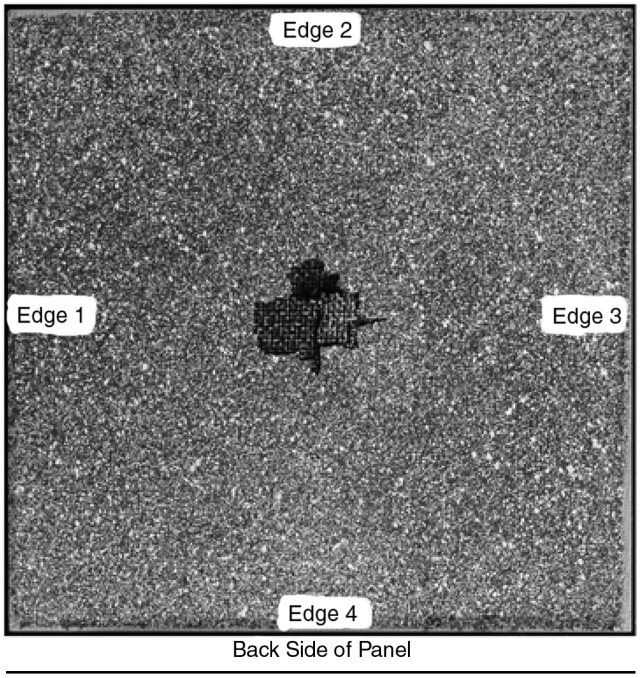

Fig. 10 Posttest photograph of the back side of a 6 × 6 in. RCC flat panel. Coating loss is evident at the center.

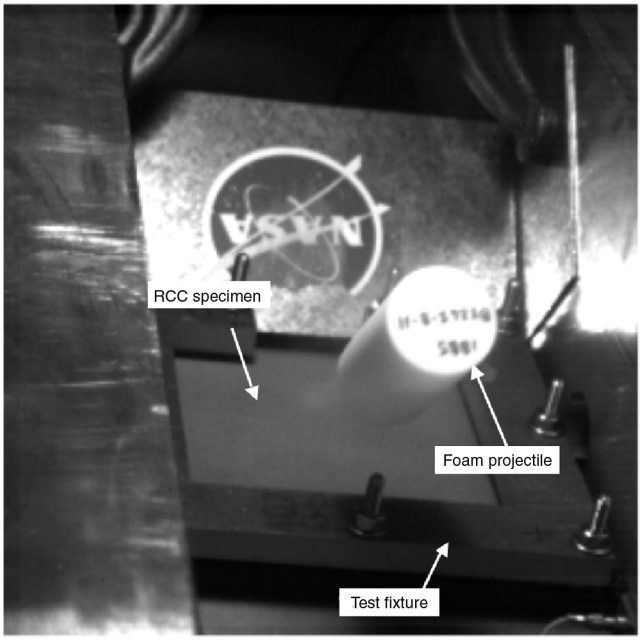

Fig. 11 Photograph of 45-deg foam impact onto 6 × 6 in. RCC plate.

displacements were constrained along three edges, as represented by the dashed lines in Fig. 12. The displacements, both out-of-plane and in-plane perpendicular to line A–A, were constrained. No rotations were constrained at the boundaries. The RCC material properties and plate thickness were adjusted for each impact to agree with test documentation. The foam projectile was modeled as room-temperature BX-265 foam using 5250 solid elements. The foam dimensions were 1.5 in. in diameter and 3.0 in. long. The density of the projectile foam was varied to match the test-specific projectile mass. The RCC material was characterized using the LS-DYNA Mat-58 material model.

C. Test-Analysis Correlation: Flat Plates

A comprehensive systematic approach was used for the test-analysis correlations. A review of the test data indicated that

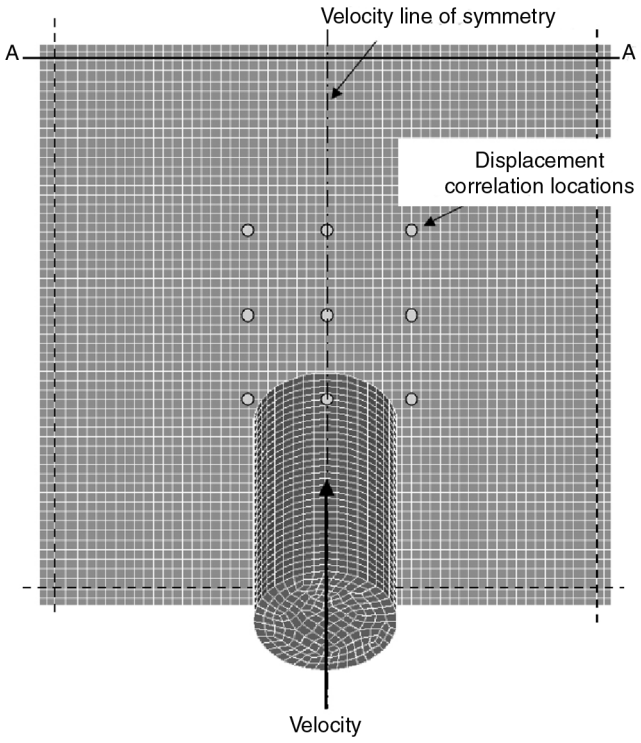

Fig. 12 LS-DYNA model of foam cylinder impacting RCC panel at 45 deg.

high-quality data were acquired. For example, the deflection data indicated that the panel responses were symmetric about the velocity line of symmetry (see Fig. 12). The quantitative correlations, shown in Fig. 13, were based on a comparison of displacements at nine locations on the panel, as identified in Fig. 12. The eight locations not at the center are 0.9 in. left or right of the center and/or 0.9 in. above or below the center. In addition to the quantitative correlations, qualitative correlations of end-state damage are shown in Figs. 14 and 15. The experimental damage is based on posttest photographs and NDE results. Analytically, the damage is presented as maximum damage parameters generated by the Mat-58 RCC model. The damage parameters represent the accumulation of damage in each of the 19 plies of the RCC material.

Detailed test-analysis correlations were performed for each test. An example of correlation results is shown in Fig. 13 for test R285_10, which occurred at 1837 ft/s. This particular test was selected because the damage is very close to the NDE-detectable limit. Several features are noted. Symmetric locations are plotted on the same figure in the left-hand column. The symmetry in the simulation is nearly ideal and therefore no distinction is discernible for the analytical results. The difference in the experimental results for symmetric locations is small, indicating that a nearly symmetric response was measured. The figures in the right-hand column show comparisons for the middle locations. The comparison of the time histories is very close for all locations.

The tests conducted at impact velocities less than 2000 ft/s did not exhibit a significant amount of NDE-detectable damage. The difference in maximum displacements between test and analysis ranged from 1 to 19%, with 75% of the comparisons having an error less than 15%. In general, the lower corners are more accurately predicted than the upper corners.

A qualitative comparison of measured and predicted damage is shown in Figs. 14 and 15. In these two figures, the first column describes test conditions, the second column shows an NDE ultrasonic image, the third column shows photographs of the test panel with the back side on the left and the front (impact) side on the right. Finally, the fourth column shows the LS-DYNA analysis contour plot of the maximum damage parameter anywhere through the thickness. The cases shown in these figures represent impact velocities above the NDE-detectable damage limit of RCC. Both test

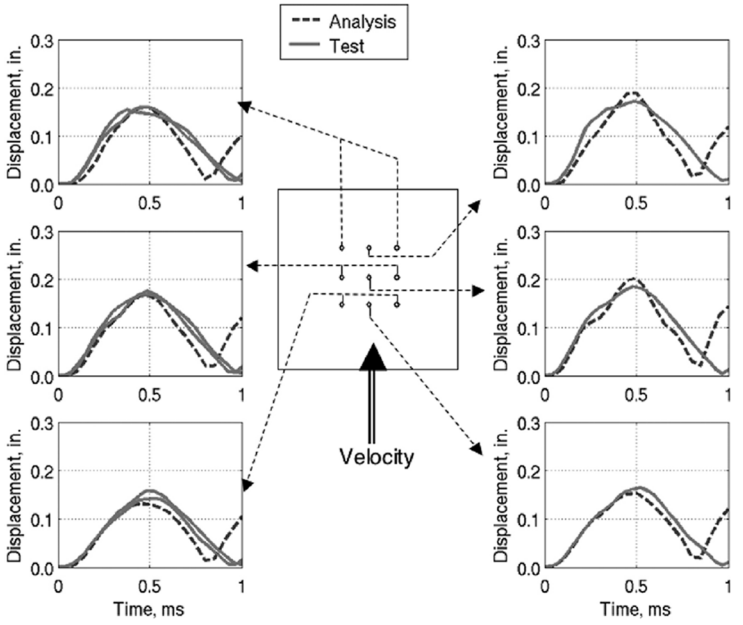

Fig. 13 Sample comparison of experimental data and analytical results for flat-plate test R285-10 at impact velocity 1837 ft/s.

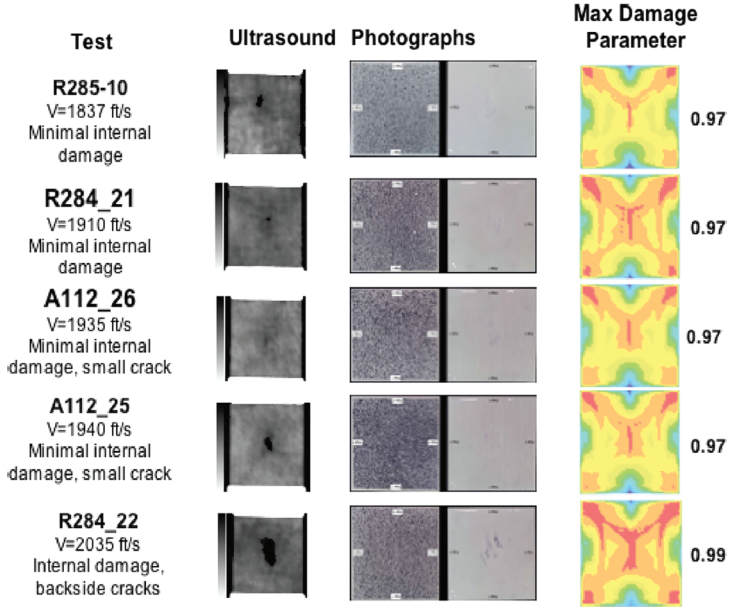

Fig. 14 Comparison of measured and predicted damage for lower velocity impacts.

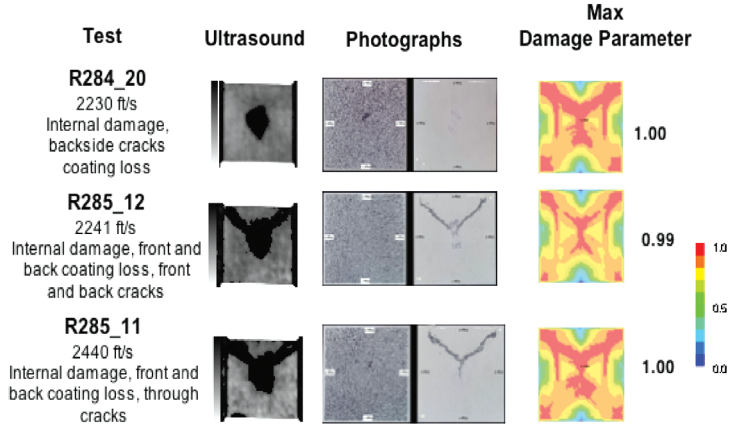

Fig. 15 Comparison of measured and predicted damage for higher velocity impacts.

and analysis indicate a similar amount of NDE internal damage for impacts ranging from 1837 to 1940 ft/s (Fig. 14). The maximum damage parameter of 0.97 correlated best with the threshold of NDE-detectable damage. For test R284-22 conducted at 2035 ft/s, the maximum damage parameter was found to be 0.99 and back-side cracks were seen in addition to the large black area of internal damage observed in the ultrasound image. At the higher velocities, both the test and analyses show significant damage to panels emanating from the center and progressing to the corners furthest from the impact site, as can be seen in Fig. 15. Note that a damage parameter of 1.0 indicates that RCC shell elements were deleted, which corresponds to a through-the-thickness crack in the test. Also, notice that the diagonal or V-shaped front-side surface damage shown in Fig. 15 follows the trends of the damage-parameter contour plots. The simulation did overpredict damage at the corners, perhaps due to overconstrained boundary conditions.

IV. Level-3 Validation Tests

Level-3 validation tests were conducted by impacting full-scale shuttle wing leading-edge RCC panels with foam blocks. Full-scale tests were conducted on panel-6, panel-8, and three different panel-9 specimens. Tests of panels 8 and 9 will be discussed in this paper. Although a complete panel is not complex geometrically, the varying thicknesses and material properties make it difficult to validate the threshold of NDE-detectable damage. Because of the wing sweep, panels 8–10 receive very high heating on reentry and degrade more rapidly than other panels. Also, the various impact locations on the panel (top surface, apex, and lower surface) must also be considered separately because they have different impact thresholds. For debris traveling down the Orbiter longitudinal axis, the maximum incidence angle is approximately 45 deg for the apex location on panels 9 though 18. The incidence angle is shallower on the upper and lower surfaces and becomes smaller as the debris moves away from the apex toward the upper and lower edges of the panel.

A. Test Setup: Panel 8

A foam-impact test onto RCC panel 8 was conducted in July 2003 at SwRI. In the test, a 1.67-lb block of foam with a cross section of 11.5×5.5 in. was shot from a large compressed-air gun and impacted panel 8 at a velocity of 777 ft/s at an angle of incidence of 25.1 deg. The primary purpose of the test was to determine if a piece of foam traveling at the estimated velocity of the foam that struck Columbia's wing could breach an RCC leading-edge panel.

The setup of panels 5 through 10 with T seals between each panel that provide a slip-side gap to allow for spar expansion and contraction is shown on the test rig at SwRI in Fig. 16. The gun barrel was rotated such that the front edge of the foam would align with the RCC panel to produce as much contact surface as possible.

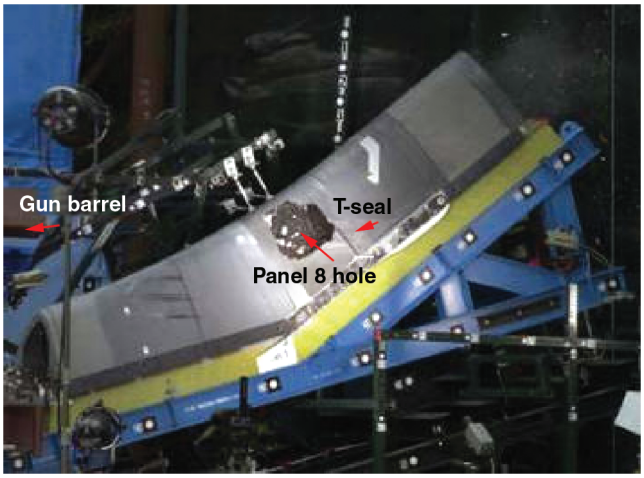

Fig. 16 Posttest photo illustrating the test setup at SwRI with panels 5 through 10 and associated T seals on the test rig.

The most obvious result from the test was the large 16×16 in. hole in panel 8, shown in Fig. 16. In addition to high-speed photographic data, photogrammetric measurements were made of the panel behind the area of the foam impact. Also, strain gauges, accelerometers, and load-cell transducers were used on the test article to obtain time histories of the impact event.

B. Model Description: Panel 8

The main shuttle Orbiter coordinate system was used for all full-scale panel impact simulations. The foam-debris velocity in the simulations was 9324 in. (777 ft/s) and was primarily along the shuttle Orbiter longitudinal axis. In 2004, Boeing Philadelphia generated LS-DYNA meshes for representative leading-edge panels and associated T seals based on information from Boeing Huntington Beach. As before, Mat 58 was used as the material model for the RCC. Because LS-DYNA does not have a Mat-58 material model for solid elements, the T seals, which act as gap sealers between panels, were modeled as shells of varying thickness.

The RCC material parameters required for the Mat-58 formulation are based on available RCC material data that were obtained by coupon-testing of laminates with various numbers of plies to failure in both tension and compression. There is a wide variation in the RCC material properties for as-fabricated material. Panels that were flown exhibit some mass loss, which further degrades the RCC material strength. In addition, the material is considerably stronger in compression than in tension. Consequently, without specific coupon tests to determine actual RCC strength for a given panel, the amount of predicted damage must be bounded by running impact simulations with the various RCC strength models. The RCC material properties for the LS-DYNA model of panel 8 obtained from coupon-testing were approximately average as-fabricated values. The failure strain for the model was approximately 0.006.

The foam model for the projectile was the LS-DYNA Mat-83 model. Strain-rate effects were found to be important in the foam material at the velocities in question. High-strain-rate data for the Fu Chang model were generated in a specially configured and instrumented 14-ft bungee-assisted drop tower at the Impact Dynamics Research Facility at LaRC that can achieve strain rates of over 400/s (see Fig. 2). The high-strain-rate data were directly input into the Fu Chang model.

The panel-8 model used to determine threshold of damage for return to flight is illustrated in Fig. 17. Each LS-DYNA-defined part is given a different color. The nominal edge length of a typical element away from the ribs is 0.2 in. The chord length of panel 8 is about 2 ft.

C. Test and Analysis Correlation: Panel 8

The damage that occurred to panel 8 during the impact test was truly catastrophic. Consequently, the primary comparisons made of the test results with analysis are the damage pattern that occurred and

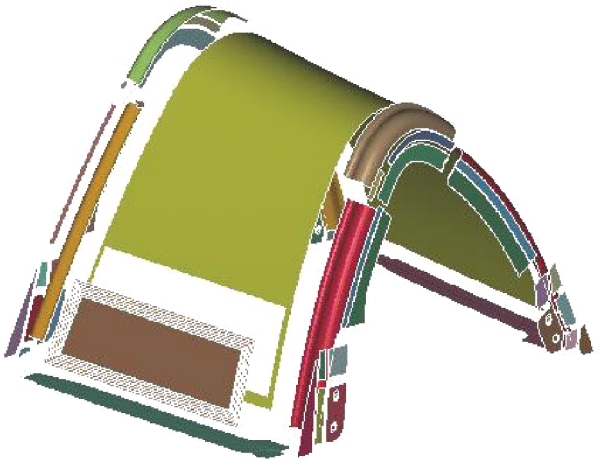

Fig. 17 Exploded view of parts of the LS-DYNA 2004 model.

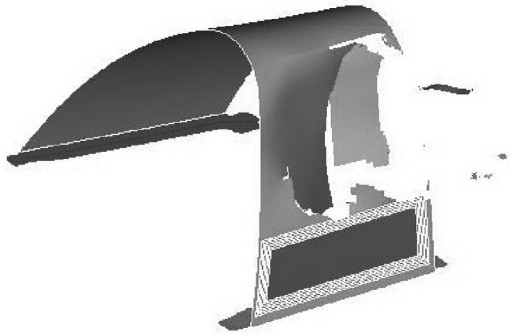

Fig. 18 LS-DYNA at 5 ms after impact (model panel ribs and foam are removed, for clarity).

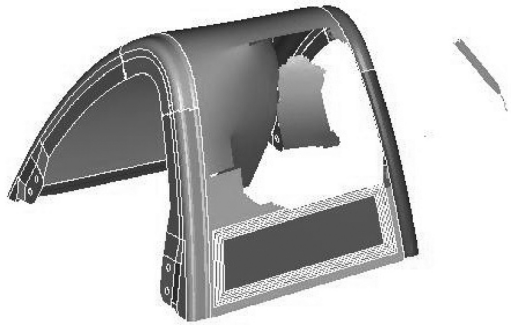

Fig. 19 LS-DYNA 2004 model showing panel damage 10 ms after impact.

photogrammetry data. The predicted damage to the panel is shown in Figs. 18 and 19, and the damage that occurred in the test is shown in Fig. 20.

The three-dimensional motion of over 100 optical targets on the inside of panel 8 were tracked using photogrammetry (Fig. 21). The motion was tracked semi-automatically using two Phantom 5 digital video cameras that captured 2000 to 7000 frames per second. The videos were analyzed by the Image Science and Analysis Group at the NASA Johnson Space Center, who examined the position and velocity of each point, looking for discontinuities in its trajectory. Spatial continuity was then assessed by comparing the motion of each point with other points in the same row and column.

Because the local axis system shown in Fig. 21 did not align with the model axes, the photogrammetric data were further processed to obtain the resultant displacement of each point vs time. Resultant displacement, a scalar quantity independent of the coordinate system, was used for the comparisons with the analysis because of the uncertainty in the coordinate transformation between the measured data and the finite element model.

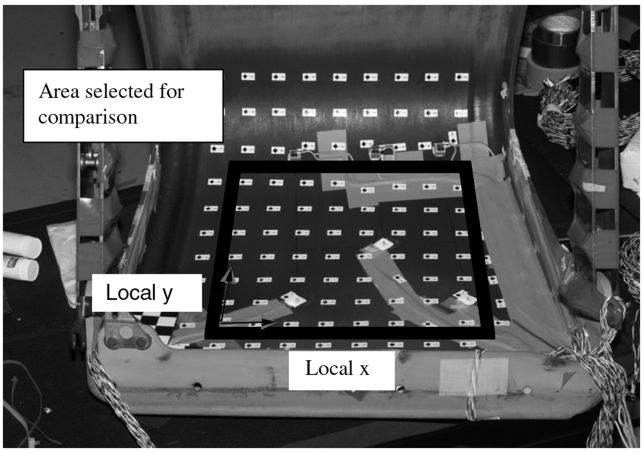

Fig. 21 Location of photogrammetric targets on panel 8 before impact. Box outlined in black indicates area of interest.

The experimental resultant displacements were then plotted as contour plots and compared with the LS-DYNA-predicted resultant displacement contours for the interval of 0.5 ms before impact until 3.68 ms after impact, which is the last data point that existed for all of the selected points. A typical comparison of test with analysis is shown in Fig. 22 at 2 ms after the foam impact.

The deflections measured using photogrammetry compare well with the analytical results and thus can be used to evaluate the simulation results up to the point at which the measured data are no longer available. It is assumed that by 3 ms, the panel had catastrophically failed. With the success of the Aramis photogrammetric system demonstrated in the level-2 testing of the 6 × 6 in. plates, full-scale panel testing also began using the Aramis system in 2004.

D. Test Setup: Panel 9

Additional level-3 testing and analysis was conducted to further validate LS-DYNA predictions of the RCC threshold of NDE-detectable damage. Panel 9 is one of the most critical panels because it is subjected to very high heating on reentry, and the incidence angle of debris traveling along the Orbiter longitudinal axis is large compared with panels 1–7 and panels 17–22. Tests were conducted using panel 9L-B to determine the threshold of damage for 0.04-lb foam debris, which is slightly above the maximum probable weight of foam debris, because the redesigned external tank was not expected to shed foam greater than 0.01 to 0.03 lb. A total of nine shots were conducted onto panel 9L-B: three along the upper surface, three along the apex, and three along the lower surface. Each test location was separated from the others by as much distance as possible, usually 4–6 in. Although nine shot locations were planned (see Fig. 23), only seven tests were actually conducted because of concerns about proximity to previous damage.

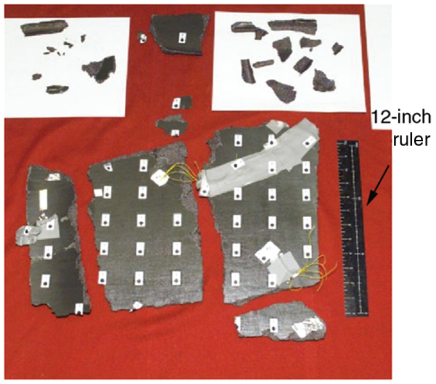

a) Fragments from panel 8

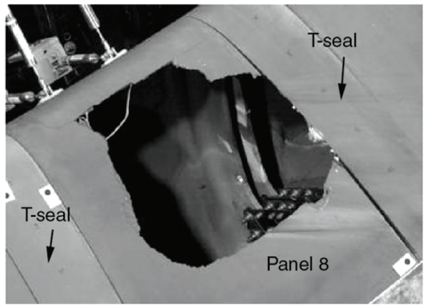

b) Panel 8 with large hole postimpact

Fig. 20 Panel debris showing a) photogrammetric targets on the back side and b) the hole in panel 8.

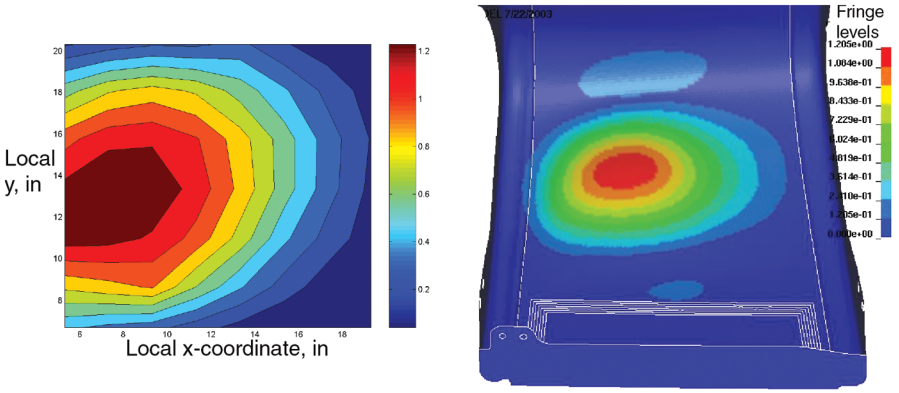

a) Measured deflection contours b) Predicted contours

Fig. 22 Comparison of a) measured and b) predicted deflections at 2 ms after foam impact. The maximum deflection contour for both plots is 1.2 in.

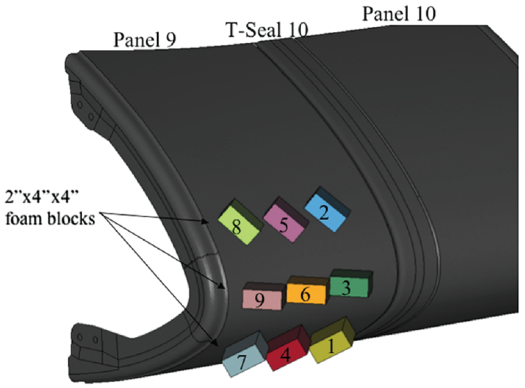

Fig. 23 Location of the nine foam-impact tests onto panel 9L-B.

For the upper and lower surfaces and apex, three impact velocities were defined using LS-DYNA predictions. The lowest impact velocity should produce no detectable damage, the middle impact velocity should have a 50% chance of producing damage such as delamination, and the highest impact velocity should produce severe damage such as a through-crack. The projectile was a block of BX-265 foam with dimensions $2 \times 4 \times 4$ in. long, weighing 0.044 lb. To account for foam density variations, the lengths of the blocks were adjusted so that the weight of each block was 0.044 lb.

E. Pretest Threshold Predictions Versus Test Results: Panel 9L-B

Because the RCC material properties of a given panel are unknown, pretest LS-DYNA predictions used minimum and maximum as-fabricated material properties to bound the amount of likely damage. In addition to material-property uncertainties, the thickness of the RCC can vary from location to location on the panel. However, because the panel-thickness variation for the 19-ply area was unknown, the thickness variation was neglected. The first three shots were planned to produce no NDE-detectable damage. Pretest simulations for tests at locations 1 (lower surface), 2 (upper surface), and 3 (apex) used minimum as-fabricated properties to ensure that no NDE-detectable damage should occur. The target velocities for no damage at locations 1, 2, and 3 were predicted to be 1150, 1000, and 950 ft/s, respectively. Because of the geometry, the apex has a lower threshold than the upper and lower surfaces, which, for a given trajectory of foam, receive a more glancing impact. The velocities achieved were 1160, 1042, and 950 ft/s. No damage of any type was observed posttest. Shots 4, 5, and 6, were designed to be at the threshold of NDE-detectable damage and thus have a 50% probability of producing detectable damage. Using a maximum damage parameter of approximately 0.9, the predicted velocities for the threshold of NDE damage were 1775, 1625, and 1375 ft/s. Note that the thresholds vary, depending on the exact location. The test velocities achieved were 1778, 1609, and 1419 ft/s, respectively. Two out of three of the tests produced damage. The most severe damage was an 8-in.-long crack with delamination that was observed at location 4 on the lower surface. At location 5 on the upper surface, there was crushed coating. However, at location 6, no damage was detected. Thus, the 50% probability of producing damage was substantiated. Next, the final shot was predicted to produce severe damage. The final shot at 1511 ft/s was at location 9 on the apex. An 8-in.-long crack with an associated 10×2 in. area of NDE-detectable internal damage was observed posttest. Testing was stopped after seven shots because panel 9L-B was so damaged that any further tests would be questionable.

V. Discussion of Results

A systematic test and analysis program was developed to validate LS-DYNA predictions of the threshold of damage to shuttle Orbiter wing leading-edge RCC panels from high-speed foam impacts. First, level-1 tests were performed to validate the separate material models of the RCC and foam. The level-1 three-point beam bending test showed that maximum damage parameters exceeding 0.9 produced NDE-detectable damage. Next, level-2 tests of foam impacts onto 6×6 in. RCC flat panels were conducted using pretest LS-DYNA predictions to determine the test velocity. The tests were conducted to produce no damage, NDE-detectable damage, and a through-crack. The LS-DYNA model was correlated with the test results, and damage parameters were monitored to assist in predicting the minimum velocity needed to produce NDE-detectable damage. A maximum damage parameter of 0.97 correlated well with the threshold of NDE-detectable damage. Although the model was developed to simulate the threshold of damage, the model was used to simulate the catastrophic damage of RCC panel 8 produced by the SwRI impact test sponsored by the CAIB. The amount of damage predicted by LS-DYNA, including the resulting 16×16 in. hole in panel 8 and the approximate shape of RCC debris, correlated well with the experiment. Finally, the threshold velocities for 0.044-lb foam impacts onto full-scale RCC panel 9L-B were predicted, and seven tests were conducted. Even without knowing exact material properties and panel-thickness variations, the test results closely matched the LS-DYNA predictions of impact damage.

VI. Conclusions

The CAIB requested that NASA determine the current capability of reinforced carbon–carbon (RCC) panels to sustain impact. Also, the CAIB suggested that NASA develop physics-based codes to more accurately simulate RCC impacts than the previous empirical models. Because RCC wing leading-edge panels are extremely expensive and are in limited supply, testing to determine the current shuttle fleet's threshold of impact damage to different types, sizes, and shapes of debris is not practical or even possible. Consequently, a program was conducted to enable relatively accurate predictions of the impact tolerance of the shuttle leading-edge wing panels using the physics-based code LS-DYNA. Accurate predictions of impact

damage from insulating foam and other debris strikes that can occur during launch required materials characterization of probable debris, including strain-rate effects. The LS-DYNA Fu Chang foam model with rate effects was used to characterize the foam material properties, and the Mat laminated composite fabric with a cumulative damage failure model was used to characterize the complex RCC material. Level-1 validation of the model was conducted for the individual foam and RCC materials. Level-2 validation was achieved by test-analysis correlation of foam impacts onto 6×6 in. flat RCC plates. Level-3 test-analysis correlation was performed on the CAIB full-scale panel-8 test. Finally, a series of foam-impact tests were performed successfully on full-scale RCC panel 9L-B using LS-DYNA-predicted velocity thresholds. The test-validated return-to-flight LS-DYNA physics-based models are now used as a predictive tool for characterizing the threshold of NDE-detectable damage for impacts of both foam and ice onto the RCC wing leading-edge panels, nose cap, and chin panel.

Acknowledgments

The work described in this paper was performed by the Reinforced Carbon–Carbon (RCC) Impact Damage Threshold Assessment Team. Special thanks go to Darwin Moon and Evelyn "Jo" Guthery of The Boeing Company, who provided direction and leadership, and to the Orbital Debris Investigation Assessment Team (ODIAT). Other individuals who deserve special mention are team members Jonathon Gabrys, Jason Firko, Josh Schatz, and Ryan Lee of Boeing Philadelphia, who developed the finite element meshes and who ran thousands of LS-DYNA simulations. We also thank Ronny Baccus of NASA Johnson Space Center (JSC), who provided hard-to-find RCC material information to the team, and Justin Kerr of JSC, who led the full-scale impact testing program. Finally, Alan Stockwell of Lockheed Martin provided excellent analysis support.

References

[1] "Report Volume 1," Columbia Accident Investigation Board, Washington, D.C., Aug. 2003.

[2] LS-DYNA, Software Package, Ver. 971, Livermore Software Technology Co., Livermore, CA, May 2007.

[3] Anon., *Reusable Launch Vehicle: Technology Development and Test Program*, National Academy Press, Washington, D.C., 1995.

[4] Carney, K., Melis, M., Fasanella, E., Lyle, K., and Gabrys, J., "Material Modeling of Space Shuttle Leading Edge and External Tank Materials for Use in the Columbia Accident Investigation," *8th International LS-DYNA User's Conference*, Livermore Software Technology Co., Livermore, CA, 2004, pp. 3-35–3-44.

[5] Melis, M., Carney, K., Gabrys, J., Fasanella, E., and Lyle, K., "A Summary of the Space Shuttle Columbia Tragedy and the Use of LS-DYNA in the Accident Investigation and Return to Flight Efforts," *8th International LS-DYNA User's Conference*, Livermore Software Technology Co., Livermore, CA, 2004, pp. C17–C24.

[6] Gabrys, J., Schatz, J., Carney, K., Melis, M., Fasanella, E., and Lyle, K., "The Use of LS-DYNA in the Columbia Accident Investigation," *8th International LS-DYNA User's Conference*, Livermore Software Technology Co., Livermore, CA, 2004, pp. 3-1–3-10.

[7] Lyle, K., Fasanella, E., Melis, M., Carney, K., and Gabrys, J., "Application of Non-Deterministic Methods to Assess Modeling Uncertainties for Reinforced Carbon–Carbon Debris Impacts," *8th International LS-DYNA User's Conference*, Livermore Software Technology Co., Livermore, CA, 2004, pp. 3-23–3-33.

[8] Fasanella, E. L., Lyle, K. H., Gabrys, J., Melis, M., and Carney, K., "Test and Analysis Correlation of Foam Impact onto Space Shuttle Wing Leading Edge RCC Panel 8," *8th International LS-DYNA User's Conference*, Livermore Software Technology Co., Livermore, CA, 2004, pp. 3-11–3-22.

[9] Lessard, W. B., "Test and Analysis of Foam Impacting a 6×6 Inch RCC Flat Panel," NASA TM 2006-214321, June 2006.

[10] Fasanella, E. L., and Kellas, S., "Quasi-Static 3-Point Reinforced Carbon–Carbon Bend Test and Analysis for Shuttle Orbiter Wing Leading Edge Impact Damage Thresholds," NASA TM 2006-214505, Sept. 2006.

[11] Matzenmiller, A., Lubliner, I. J., and, Taylor, R. L., "A Constitutive Model for Anisotropic Damage in Fiber-Composites," *Mechanics of Materials*, Vol. 20, No. 2, 1995, pp. 125–152.

[12] Schweizerhof, K., Weimar, K., Munz, Th., and Rottner, Th., "Crashworthiness Analysis with Enhanced Composite Materials Models in LS-DYNA: Merits and Limits," *5th International LS-DYNA User's Conference*, Livermore Software Technology Co., Livermore, CA, 1998.

G. Agnes
Associate Editor